Shock waves in liquid helium

A. Yu. Iznankin and L. P. Mezhov-Deglin

Institute for Solid-State Physics of the USSR Academy of Sciences
(Submitted 9 September 1982)
Zh. Eksp. Teor. Fiz. **84**, 1378–1390 (April 1983)

The formation and evolution of the profiles of plane and spherical shock waves of the first and second sounds in liquid helium, excited by a source of short and intense heat pulses, have been investigated experimentally. At an intensity below some critical value, the evolution of the shape of plane compression waves for the first and second sounds is described similarly to the way it is done in the book "Fluid Mechanics" by Landau and Lifshitz. If the intensity exceeds the critical value the shape of the recorded pulses is strongly distorted for two reasons: on account of additional damping of the pulses inside the volume, and owing to a change in the heat transfer mechanism at the solid-liquid interface. The evolution of the shape of spherical waves of first sound and of waves of second sound below 1.88 K is also in qualitative agreement with the predictions of Ref. 1. At temperatures above 1.88 K the compression and rarefaction shock fronts move toward each other in a spherical shock wave of second sound. This case has not yet been discussed theoretically.

PACS numbers: 67.40.Mj, 67.40.Pm, 43.35.Lq

I. INTRODUCTION. FUNDAMENTAL THEORETICAL CONCEPTS

We have investigated the relaxation of perturbations which appear in liquid helium when pulsed energy is released from a low-inertia heater. In recent years the interest in this problem has increased significantly, owing to two circumstances. First, to the need to make sense of the phenomena which take place when stored energy is released into the helium in pulses, e.g., by jumps in the magnetic flux in superconducting devices, in avalanche recombination of atoms of molecular gases at the surface of semiconductors by means of laser pumping, etc., and second, in connection with the development of the theory of nonlinear processes in condensed media.

Liquid helium is an ideal model object for the study of the dynamics of nonlinear waves. In addition to the waves of the usual first sound (density waves), a heater placed in superfluid He II will emit waves of second sound (entropy waves),[1] with a propagation speed which depends strongly on the temperature and tends to zero as $T \to T_\lambda$. Naturally, above the temperature T_λ only first sound waves propagate in the normal fluid, and the thermal equilibrium in the liquid near the heater is slowly restored on account of the usual diffusive heat transfer.

The velocity of propagation of the points on the profile of a finite-amplitude sound wave differs from the acoustic speed which is computed assuming infinitely small amplitudes. The deformationof the profile of a traveling wave can lead to the development of discontinuities (of the density ρ or pressure p for the first sound, and of the temperature T for the second sound), i.e., to the formation of shock waves in the fluid if the power of the source of disturbances is large enough.[1]

Osborne[2] was the first to observe second-sound shock waves of liquid helium. The theoretical calculations of the velocity of motion of a plane traveling second sound wave and of the speed of propagation of temperature discontinuities in He II was carried out by Khalatnikov.[3] Subsequent experimental papers were devoted to the study of the dependence on the temperature of the bath and the power of the source of the velocity of motion of a finite-amplitude wave,[4] or of a plane second-sound shock front,[5,6] i.e., in fact to a test of the domain of applicability of Khalatnikov's calculations. Gulyaev[7] describes qualitative observations of the propagation of plane and cylindrical waves in helium by means of the dark-field method.

In distinction from Refs. 4–7, we have observed the change of the shape of the profile of shock waves in first and second sound propagating in liquid helium at temperatures between 1.3 and 3.5 K, produced by plane or pointlike sources of pulsed disturbances (the power in a pulse was up to 50 W, the duration 0.1–10 μs). In other words, we have studied the evolution of plane and spherical first and second sound waves as a function of the power of the emitter, the temperature of the bath, and the distance traversed by the wave. Some preliminary results were published earlier.[8–11]

The methods for calculating the speed of propagation of the points of the profile of a one-dimensional first or second sound wave of finite amplitude moving away from the source are similar (Ref. 1, Secs. 94, 95, 130 of the Russian edition; Secs. 94, 95, 131 of the 1959 English edition; Translator's note). In first approximation the velocity of a point of the profile of a first sound wave with amplitude $\delta\rho$ is

$$u_1 = u_{10} + (\partial u_1/\partial \rho)\,\delta\rho \approx u_{10} + \alpha_1 v;$$
$$v = \int \frac{u_1}{\rho}\,d\rho = \int \frac{dp}{\rho u_1}, \qquad \alpha_1 = \frac{u_1^4}{2V^3}\left(\frac{\partial^2 V}{\partial p^2}\right)_s, \qquad (1)$$

where u_{10} is the acoustical velocity of the first sound, ρ is the density, α_1 is the nonlinearity coefficient, V is the specific volume, p is the pressure, and v is the velocity of flow of the fluid at the given point of the profile.

Similarly, one can write for the velocity of displacement of a second sound plane wave to first approximation[1,3,10]

$$u_2 \approx u_{20} + (\partial u_2/\partial T)\,\delta T. \tag{2}$$

Neglecting the terms which contain the derivative $\partial \rho/\partial T$, i.e., for temperatures not too close to the critical T_λ, Eq. (2) can be simplified [Ref. 1, Sec. 130 (Russian) = 131 (English) and Refs. 3, 4, 10]:

$$u_2 \approx u_{20} + \alpha_2 v_n, \tag{3}$$

$$\alpha_2 = \frac{TS}{C_v}\left[\frac{\partial}{\partial T}\ln\left(\frac{u_{20}{}^3 C_v}{T}\right)\right], \qquad v_n = \int \frac{u_2}{S}\, dS,$$

where C_v and S are respectively the heat capacity and entropy per unit volume. If the heat flux density Q is known, then $v_n = Q/TS$. The quantity α_2 has been measured in Ref. 4, and in the monographs[3,12] one can find the graph of $\alpha_2(T)$.

In distinction from first sound waves, where $\alpha_1 > 0$ (the derivative $\partial u_1/\partial \rho > 0$), the sign of the coefficient α_2 depends on the temperature of the liquid: it is positive in the region $1 < T < 1.88$ K and negative for $T > 1.88$ K, so that large-amplitude second sound compression waves ($T > 0$) will either overtake or lag the acoustic second sound waves, depending on the temperature of the bath. As a result, second sound shock waves (temperature discontinuities) will be formed in superfluid He II either at the wave front, as in the ordinary sound, or, for $T > 1.88$ K, on the decline of the traveling one-dimensional compression pulse. The speed of the shock front in the medium is the arithmetic mean of the speeds of the profile on both sides of the discontinuity surface[1], i.e., is equal to $u_{12} + (1/2)\alpha_1(v^{(1)} + v^{(2)})$, or

$$u_{20} + {}^1/_2\alpha_2\,(v_n^{(1)} + v_n^{(2)}). \tag{4}$$

Khalatnikov's theory[3] considers only weak one-dimensional (plane) second sound shock waves. As was shown by measurements,[4–6] the computed arrival time of a second sound pulse is in good agreement with the experimental value for a power density in the perturbing pulse $Q \leqslant 15\,\mathrm{W/cm^2}$ and a pulse duration τ of the order of ten microseconds (when τ is decreased to 2 μs agreement is found up to $Q = 100\ \mathrm{W/cm^2}$ Ref. 6). For $Q > 15\ \mathrm{W/cm^2}$ and $\tau = 50\ \mu$s there is strong disagreement between theory and experiment, but until now the reason for these discrepancies has not been established in an unambiguous manner.

The propagation of shock fronts of arbitrary shape (in particular, spherical fronts) in second sound has not been investigated theoretically, although in real experiments the shape of the front may differ considerably from a plane. This may be one of the reasons for the discrepancies between theory and experiment. If the temperature discontinuities of arbitrary shape may serve as sources for vortices in He II, similar to the strong discontinuities in a classical fluid[1,12], then the original Khalatnikov equations[3] require corrections. We note that when second sound spherical waves propagate in He II at a temperature higher than 1.88 K there arises a problem unknown in classical fluid dynamics: the opposing motions of compression and rarefaction shock fronts that follow directly one after the other in the divergent wave.

As will be seen from the sequel, it would be interesting to carry out a theoretical investigation of the problem of possible appearance of vortices at the solid-liquid interface for pulsed heating of the surface, and in general of the peculiarities of the heat (transfer at the interface at large power, as well the evolution of the shape of a second sound pulse in the presence of vortices in the liquid and the problem of damping of shock waves for a bath temperature below 0.9 K, when the density of the normal component falls off rapidly (shock waves below 1 K have not been studied experimentally). There has been no theoretical investigation of the peculiarities of propagation of strong shock waves of first sound in liquid helium.

II. THE MEASUREMENT METHOD

The experimental installation is shown schematically in Fig. 1. A low-inertia film source of thermal pulses, the heater H and a low-inertia thin-film receiver of thermal oscillations (superconducting bolometer), have been placed in the liquid at distances varying between 0.06 and 8 cm. The area of the heater (a bismuth film of 10^{-4} cm thickness) ranged from 2 $\mathrm{cm^2}$ to 3 $\mathrm{mm^2}$ in various experiments. The characteristic size of the receiver (consisting of an indium or tin strip of 10^{-4} cm thickness) was in most experiments 3×1 mm. This allowed us to realize in various experiments a geometry which ranged from one approaching plane geometry (flat source-point receiver) to one which was almost spherical (point source with receiver at a large distance).

In the normal state the resistance of the bismuth film and of the indium or tin strip was of the order of tens to hundreds ohm, and the width of the superconductive transition region of the bolometer film was on the average in the tenth of a kelvin. The working temperature could be set in the interval 1.3–3.4 K by varying the magnetic field in the superconducting solenoid S.

The films were sputtered onto the surfaces of plane polished quartz glass disks of 2 cm diameter in the early experiments and of 6 cm diameter in the later ones. The smaller diameter disks were placed inside the solenoid which, was cooled by liquid helium. The distance between the disks was determined by the thickness of ring-shaped shims and was chosen to be 0.06 cm, 0.3 cm, and 1 cm. The liquid helium was freely flowing into the measuring cell through openings in the shims. The disks of 6 cm diameter were placed inside a cylindrical stainless steel beaker as shown in Fig. 1. A shaft

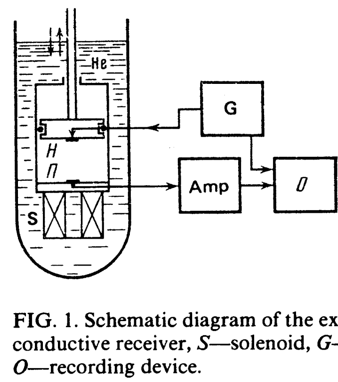

FIG. 1. Schematic diagram of the experimental setup: H-heater, -superconductive receiver, S—solenoid, G—pulse generator, Amp—amplifier, O—recording device.

passing through the top of cover of the beaker made it possible to displace the upper heating disk along the vertical, relative to the fixed receiver. The superconducting solenoid S was placed below the bolometer.

The external devices consisted of a reactangular pulse generator G, a low-noise pulse preamplifier and broadband amplifier Amp, as well as a recording device O consisting of a stroboscopic oscilloscope for visual observations and photographing of the display. In the stroboscopic regime the periodic pulses of duration $\tau = 0.1$–$10\,\mu$s and maximal power up to 50 W with a repetition rate of 5–40 Hz were fed to the heater and at the same time triggered the oscilloscope sweep. The recording device could follow the shape of the temperature pulses of amplitude $T \geqslant 10^{-5}$ K and a slew rate to 0.3 μs. The characteristic time for the transformation of a temperature pulse into an electric pulse at the liquid-helium bolometer interface, determined essentially by the product of the heat capacity of the film and the Kapitza thermal resistance at the interface, was negligibly small (smaller than 10^{-7}s), so that the shape of the recorded signal was determined by the properties of the medium in which the pulse propagated as well as by the transients at the heater-liquid interface. If, for instance, at large Q bubbles which appear in the normal component layer near the surface on account of temperature fluctuations manage to fuse together within the duration τ of the pulse, then the nucleate boiling is changed into film boiling. It is known that in the static regime the critical power sufficient for film formation around the heater is $Q_c = 0.1$–$1\,\mathrm{W/cm^2}$. In the pulsed regime Q_c depends on the duration of the pulses and according to measurements[13] at 4.2 K and $\tau = 10^{-2}$–10^{-4} s is close to

$$Q_c\,[\mathrm{W/cm^2}]=0.2\tau^{-0,5}, \tag{5}$$

i.e., for $\tau = 10^{-6}$ s we have $Q_c \approx 200\,\mathrm{W/cm^2}$. As the temperature is lowered the magnitude of Q_c seems to decrease. We shall return to the question of gas film formation when we discuss the results of observing high-power pulses.

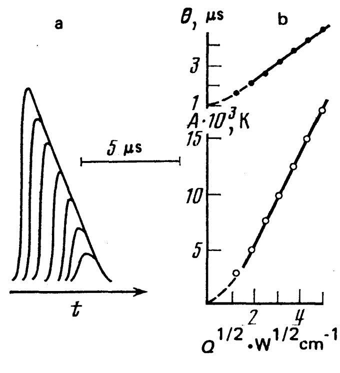

FIG. 2. The dependence of the shape of the recorded plane compression waves of second sound ($\delta T > 0$) on the power Q of the exciting pulses of duration 1 μs for $T = 1.79$ K, with the coefficient $\alpha_2 > 0$. The emitter-receiver distance was $L = 0.92$ cm. The figure a represents the evolution of the shape of the recorded pulse as Q increases; the figure b shows the dependence of the amplitude A and the width θ of the same pulses as a function of $Q^{1/2}$.

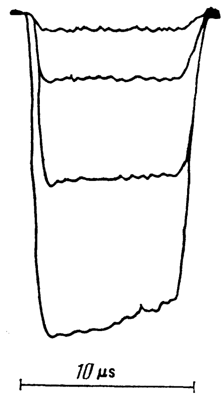

FIG. 3. The shape of plane compression waves of second sound for T. $T = 1.88$ K, where $\alpha_2 \approx 0$. The duration of the pulse is $\tau = 10\,\mu$s, $Q = 1.6$, 6, 14, and 25 W/cm^2.

III. SECOND SOUND SHOCK WAVES

1. Plane waves

Typical diagrams showing the evolution of the shape of the recorded pulses as the power Q is increased in a cell with a plane heater of area 2 cm^2 and a pointlike receiver, at a emitter-receiver distance $L = 0.9$ cm, are shown in Figs. 2–4. The duration of the exciting rectangular pulse was $\tau = 1$ μs in Fig. 2 and 10 μs in Figs. 3 and 4. According to what was stated in the Introduction, for $T < 1.88$ K, when the nonlinearity coefficient α_2 is positive, a shock wave is formed along the front of the propagating pulse, whereas for $T > 1.88$ K a shock is formed on the decline of the pulse; near the point where α_2 goes through zero the shape of the recorded pulses varies little with the variation of Q and is close to the shape of the emitted pulse (Fig. 3).

The dependence of the amplitude A and width θ of the recorded pulse on the power of the emitted pulse is shown in Fig. 2,b and Fig. 4,b. The difference in the durations of the initial pulses allows one to distinguish clearly two sections.

1. For wide emitted pulses the shape of the recorded pulses is close to a rectangular trapezoid. In this case the amplitude A of the pulse and the difference $\theta - \tau(\theta$ is the

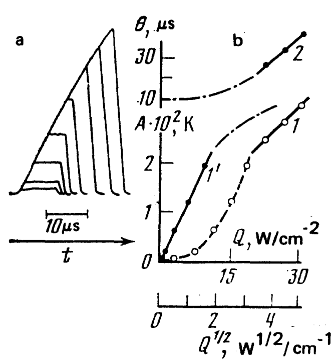

FIG. 4. The dependence of the shape of the recorded pulses on Q for 2.0 K, where $\alpha_2 < 0$. The duration was $\tau = 10\,\mu$s, and $Q = 0.6$–25 W/cm^2; the figure a shows the evolution of a rectangular pulse; the figure b illustrates the dependence of the amplitude A and width θ on $Q^{1/2}$ (curves 1 and 2) and the dependence of A and Q (curve 1′).

width of the base of the trapezoid, τ is the width of the original pulse) increase in proportion to Q.

2. Narrow initial pulses, the shape of the recorded pulse being a right triangle: the altitude A and the base θ of the triangle increase as $Q^{1/2}$. It is easy to derive these dependences making use of simple geometric constructions, similar to the ones in the monograph[1] and in the Ref. 6.

As can be seen from Fig. 2, for $\tau = 1\ \mu s$ and $Q \gg 1$ W/cm^2 the dependence of A and θ on Q are close to a square root, i.e., a triangular profile will appear at a distance much smaller than the width $L = 0.9$ cm. This coincides with the results of observations for small distances $L = 0.06$ and 0.3 cm.[8,9]

It follows from Figs. 2–4 that for $\tau \leqslant 10\ \mu s$, $Q \leqslant 25$ W/cm^2, and $T < T_\lambda$ (in reality $T \leqslant 2.0$ K) the evolution of the profiles of plane pulses of second sound agrees well with the predictions based on Khalatnikov's theory. The third section of this chapter is devoted to a discussion of the results of measurements at large power levels. The evolution of the shape of second sound waves near the lambda-point T_λ, where the simple formula (3) is no longer valid for computing the velocity u_2 and where one cannot neglect the damping of the second sound wave, also requires a separate investigation.

2. Spherical shock waves

In a narrow cell with plane-parallel walls one can observe multiply reflected second sound pulses, with a free path in the liquid exceeding by a factor of three, five, ect., the width L of the cell. This allows one to obtain a qualitative picture of the evolution of the shape of an isolated pulse at large distances from the emitter. It turned out[8–11] that right behind the compression wave ($\delta T > 0$) one observes in the reflected pulses a rarefaction wave ($\delta T < 0$), whose amplitude after two or three reflections in a cell of width $L = 0.9$ cm becomes equal to that of the compression wave (a similar behavior can be seen in Figs. 7, b, c, below).

According to Landau[1] this can be related to the curving of the shape of the wave front of a propagating wave at large distances from the source, since at $L \gg d$ (the characteristic diameter of the emitter) the shape of the front of the traveling wave approaches a spherical one, and in a diverging spherical acoustic wave the compression wave is followed by a rarefaction wave. To test this prediction we have installed near the emitter of area 4 cm^2 a copper screen with an opening of 2 mm diameter, and have compared the shapes of the pulses recorded by the bolometer placed at a distance of $L = 2$ cm before and after the installation of the screen. In the first case the amplitude of the rarefaction wave was insignificant in the original and first reflected pulse, and in the second case it was close to the amplitude of the compression wave.

The physical reason for the production of a rarefaction wave in spherical first sound waves produced by a pointlike disturbance is clear: The area of the wave front increases as r^2, r being the distance from the source, and the amplitude of the particle velocities in the wave decreases as $1/r$. Hence, conservation of matter in the wave requires a compensation of the increase of mass in the compression wave region on account of the rarefaction in the region following right behind it.[1]

A similar discussion can be carried through for second sound waves (entropy waves)[9], which propagate according to the equation

$$\frac{\partial^2 \psi}{\partial t^2} = u_2^2 \Delta \psi,$$

where the quantity ψ is related to the variation of the temperature and of the velocities of the normal and superfluid components by the following relations

$$\delta T = \partial \psi / \partial T, \quad P/S = \nabla \psi.$$

Here $P = \rho_n (v_s - v_n)$ is the momentum of the relative motion, and S is the entropy. Like in density waves of ordinary sound, the amplitude of the relative momentum varies as $P \propto 1/r$. Therefore, for conservation of entropy flux, which is proportional to $4\pi r^2 P$, it is necessary that the increase in the quantity of normal component (of entropy or of temperature) in a compression wave be compensated by an inflow from the region following behind the compression (temperature increase) wave, thus leading to the formation of a shallower rarefaction (cooling) wave in the region behind the compression wave.

For large emitted intensities it is natural to expect that both a compression shock wave and a rarefaction shock wave will appear. The shape of the profile of a spherical wave of ordinary sound can be found in Ref. 1, §95. Discontinuities of the densities are formed on the front of a compression wave, and on the decline of a rarefaction wave (we recall that $\alpha_1 > 0$), but in distinction from compression waves, the particle velocity is not zero in the region behind the discontinuity in a rarefaction wave and tends asymptotically to zero as $r \to 0$.

There have been no theoretical investigations of the propagation of spherical second sound waves in He II. It is understood that at $\alpha_2 > 0$ the shape of a second sound wave must be similar to the evolution of a first sound wave, but at $\alpha_2 < 0$ the shock fronts move against each other, and the analogy breaks down.

In order to create a geometry close to spherical, we have decreased the size of the heater in the cell shown in Fig. 1 to 3×3 mm and have carried out the measurements at distances $L \geqslant 1$ cm. The decrease of the area of the emitter allowed us to raise the maximal power density in a pulse to $Q = 600$ W/cm^2. The evolution of the shape of a pulse as the distance increases for temperatures $T = 1.4$ and 1.97 K is shown in Fig. 5. The duration of the perturbing pulse was $\tau = 0.1\ \mu s$, the power density was $Q = 500$ W/cm^2. It can be seen that temperature discontinuities in the wave occur at considerably larger distances from the source than in compression waves. For $T > 1.88$ K the temperature jump occurs in the middle of the travelling wave. For $T < 1.88$ K the pulse profile is close to the one given in Ref. 1. However, the width of the rarefaction wave is close to the width of the compression wave, and behind the compression wave follows again a small-amplitude compression wave, in distinction from Ref.

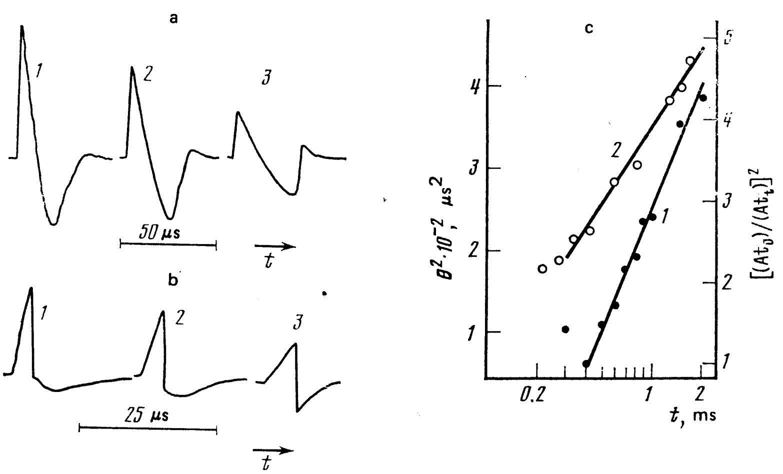

FIG. 5. The evolution of the shape of a second sound wave propagating from a source of small size 3×3 mm as a function of the distance from the emitter. The formation of a rarefaction shock wave ($T<0$) in a spherical wave ($Q=500$ W/cm^2, $\tau=0.1$ μs): a) $T=1.4$ K, $\alpha_2>0$, $L=0.44$ cm (curve 1), 0.68 cm (curve 2), and 1.2 cm (curve 3); b) $T=1.97$ K, $\alpha_2<0$, $L=04.$ cm (curve 1), 0.58 cm (curve 2), and 1.12 cm (curve 3); c) the dependence of the amplitude A (curve 1) and width θ (curve 2) of a compression shock wave of second sound ($\delta T>0$) on the propagation time t of a divergent wave in the liquid at $T=1.41$ K (1 ms corresponds to $L=2$ cm).

1, where the velocity in the rarefaction wave tends asymptotically to zero as $r\to 0$.

The calculations of Ref. 1§95 show that at large distances the amplitude of a compression wave decays $A\propto(1/r)[\ln(r/a)]^{1/2}$, and its width increases: $\theta\propto[\ln(r/a)]^{1/2}$ (here a is a constant with the dimension of length). When one changes the distance in the experiment it is more convenient to measure the arrival time $t=L/u_2$ of the pulse rather than the distance L. The dependence of the quantities $(At)^2$ and θ^2 on $\ln t$ for compression waves at $T=1.4$ K is shown in Fig. 5,c. To the time $t=1$ ms corresponds a distance $L=2$ cm. It is clear that for $t\geqslant 0.4$ ms the experimental data lie on straight lines, i.e., the change of shape of the compression wave for $\alpha_2>0$ agrees with the predictions of Ref. 1. For $T=1.97$ K the points are not on a straight line in the indicated coordinates. Apparently the interaction of compression and rarefaction shock waves leads to additional damping of the amplitude and to a decrease of the width of the compression wave.

The shape of the profile of a spherical wave changes drastically when the sign of α_2 changes. This can be used for the determination of the point T_s where $\alpha_2=0$. When the bath temperature equals T_s then $\alpha_2<0$ in the compression wave and $\alpha_2>0$ in the rarefaction wave, so that in both waves the discontinuities are formed on the decline of the pulse (Fig. 6) and both discontinuities move in the same direction in a comoving coordinate frame. According to our measurements $T_s=1.883\pm 0.008$K, in good agreement with data of other authors.[4-6]

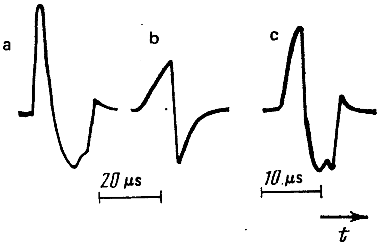

FIG. 6. The evolution of the shape of a spherical wave with shock fronts of compression ($T>0$) and rarefaction ($\delta T<0$) near the point where the coefficient α_2 passes through zero ($Q=500$ W/cm^2, $\tau=0.1$ μs, $L=2$ cm): a) $T=1.868$ K, b) $T=1.92$ K, c) $T=1.883$ K.

3. Large-amplitude shock waves

While investigating the dependence of the shape of second sound plane waves in narrow cells on the power of the exciting pulse we have observed distortions of the shape for $Q>30$ W/cm^2 and $\tau=10$ μs.[8,10] It was already noted by Vinen[14] that this could be caused both by the superposition of reflected and exciting pulses in periodic excitations, and the buildup of eigenmodes in the plane-parallel resonator and the appearance of an additional damping in the volume at large power levels. In addition, a distortion of the pulse shape could be due to a change in the heat transfer regime at the interface between the source and the liquid, as a result of the formation of a gas film.[13]

Increasing the gap from 0.06 to 1 cm significantly decreased the interference between reflected and emitted pulses as well as the amplitudes of the eigenmodes. We have therefore repeated the measurements of the damping of second sound waves at large power levels in a wider cell, at the same time increasing the distance between the emitter and receiver to 1.5 cm. The area of the heater in this series of experiments was 1.1×1.1 cm, so that the shape of the front of the pulse reaching the bolometer was closer to a plane than a sphere.

When recording in a stroboscopic regime with a scan rate of 40 Hz, the amplitude of the pulses increased initially with Q, as usual, but at $Q\geqslant 18$ W/cm^2 we observed a jumplike decrease of the amplitude. The dependence of the pulse shapes on Q for $T=1.74$ K is shown in Fig. 7,a. As the repetition rate of the pulses decreases the amplitude and the width of the last pulse gradually approached the calculated value. This behavior could be explained by the accumulation in the volume of vortex rings whose concentration varied little over a time of the order of one millisecond, but became

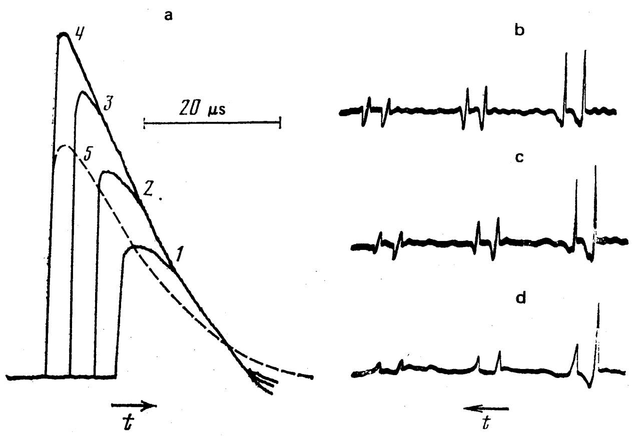

FIG. 7. The distortion of the shape of second sound pulses emitted by a plane source of area 1.1 × 1.1 cm for power levels above the critical level: a) oscilloscope traces of a single periodically repeated pulse in stroboscopic regime for $T = 1.74$ K ($\tau = 10\,\mu$s, $L = 1.6$ cm, repetition rate 40 Hz) $Q = 4.4$ W/cm^2 (curve 1), $Q = 7$ W/cm^2 (curve 2), $Q = 12$ W/cm^2 (curve 3), $Q = 14$ W/cm^2 (curve 4), and $Q = 17.5$ W/cm^2 (curve 5); the traces b, c, and d shows the evolution with increasing Q of an exciting pulse followed after 300 μs by a test pulse of identical initial power $Q = 10$, 15, and 20 W/cm^2, respectively, and a duration of $\tau = 10\,\mu$s. The temperature of the bath was 1.4 K, $L = 1.5$ cm, and the registration was stroboscopic.

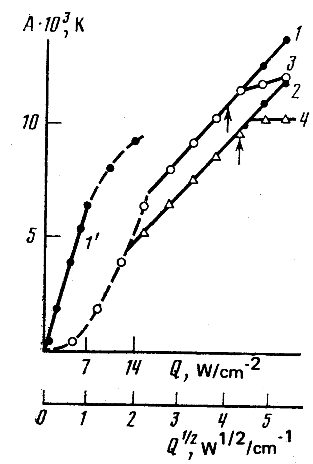

FIG. 8. The dependence of the amplitude of the exciting pulse (curves 1, 2) and testing pulse (curves 3, 4) of second sound as a function of $Q^{1/2}$ in the single-firing regime at $T = 2.005$ K, in the same cell as in Fig. 7 b. The duration of the initial pulses was $\tau = 10\,\mu$s (curves 1, 1′, 3) and 6 μs (curves 2, 4); the arrow indicates the power threshold beyond which the first sound is observed.

negligible after a time of the order of a few seconds, in agreement with the results of the investigations of Ref. 14.

In order to estimate the characteristic time of damping of the vortices we have changed the strategy of the experiment: we have studied the damping of paired pulses—an "exciting" one and a "testing" pulse, following each other at time intervals ranging from tenths of a microsecond to 20 seconds. The duration and power of both pulses were identical. Oscillogams which illustrate the change of the shape and amplitude as Q increases, recorded in the stroboscopic regime, are shown in Fig. 7, b, c, d. The bath temperature was 1.4 K, the length of the pulses $\tau = 10\,\mu$s, the time interval between the pulses was 300 μs, the repetition rate was 40 Hz. Right after the main pulse one can see the arrival of the first and second reflected pulses. It is clear that as the power is raised from 10 to 20 W/cm^2 the amplitude of the test pulse decreases by more than a factor of three compared to the amplitude of the exciting pulse.

In the single firing regime the test pulse of power 20 W/cm^2 was considerably less damped, but it was still possible to tell the difference between the amplitudes of the exciting and test pulses for delay times between the pulses ranging from hundreds of microseconds to several seconds. An example of the dependence of the amplitudes of the exciting and testing pulses of duration 10 μs (the family of curves 1, 3, 1′) and prime 6 μs (the curves 2, 4) on the power in the single-firing regime is shown in Fig. 8. The testing pulse followed 300 μs after the exciting pulse. We remind the reader that in the stroboscopic regime the same test pulse of duration $\tau = 10\,\mu$s was damped by a factor of three compared to the exciting pulse for $Q = 17.5$ W/cm^2. The damping of a test pulse of 42 W/cm^2 power and 20 μs duration, following after an exciting heat pulse propagating in a direction perpendicular to that of the testing pulse was observed in the recently published paper.[15]

Qualitatively the results of our paper and of Ref. 15 agree with the results of Vinen's paper[14]:

1) the threshold power for the formation of vortices in the unperturbed superfluid increases with the decrease of the exciting pulse;

2) in the presence of vortices in the liquid (periodic disturbances, paired pulses of high power) the threshold power decreases;

3) the characteristic decay time of the vortex structure is of the order of tens of seconds.

It does not make much sense to carry out a quantitative comparison with Ref. 14, in view of the widely different durations of the exciting pulses (Vinen was working with practically stationary fluxes).

The appearance of vortices could explain the deviation of the arrival time of the shock front of a second sound compression wave from the theoretical calculations based on the Khalatnikov theory, reported in a series of papers (e.g.,[5,6]).

After the publication of Ref. 14 it has become traditional in the literature to discuss the probability of vortex formation as a consequence of thermal fluctuations in a large-amplitude wave,[16] but one can propose several other mechanisms for vortex formation: a) as a consequence of energy dissipation in the region of a strong temperature discontinuity[12]; b) vortex formation on account of friction at the liquid-solid interface; c) vortex formation through the generation of bubbles at the heater (in Fig. 8 the arrows point to power levels above which we have also recorded strong first sound waves which, as will be shown in the next section, are emitted as a consequence of the formation of a gas film on the heater). However, now it is hard to give preference to one vortex formation mechanism over the others.

IV. FIRST SOUND SHOCK WAVES

For temperatures $T > 1.8$ K and $Q > 10$ W/cm^2 the bolometer has recorded the arrival of pulses propagating with the speed of first sound,[8] in addition to the second sound pulses. It is clear that in the experiment one measures the temperature distribution in a quasiadiabatic first sound wave.

According to the Maxwell relation

$$\delta T=\delta p(\beta TV/C_p), \quad (6)$$

where C_p is the heat capacity per unit volume of the liquid. The thermal expansion coefficient β of liquid helium in the temperature range 1.8–3.4 K is sufficiently large, on the average ($|\beta| \sim 10^{-2}$ K^{-1}) and changes sign at the maximal density point, which is situated somewhat above T_λ. Since the temperature region near T_λ will not be discussed here, one may assume that $\beta > 0$ above T_λ and accordingly $\beta < 0$ below T_λ, so that in a plane compression wave δp and δT will be positive in the normal helium whereas $\delta p > 0$ and $\delta T < 0$ in supefluid He II. The sign change of β at low temperatures is observed not only in helium, but also, for instance, in water near the freezing point. However, the recording of the profile of traveling waves in normal substances by means of temperature transducers is difficult, since the ratio $\beta T/C_p$ for such substances is smaller by several orders of magnitude than in liquid helium.

Judging by the results of our measurements, the bolometer recorded the sound waves which appeared from the formation of a gas film around the heater at large values of Q. If the second first sound plane wave would be formed as a consequence of the heating of a layer of liquid near the heater, then according to Eq. (6), a compression wave (δT, $\delta p > 0$) should be formed in the normal liquid, and a rarefaction wave ($\delta T > 0$, $\delta p < 0$) should appear in the superfluid He II. The amplitudes of the temperature oscillations in the first sound wave in He II must be much smaller than the amplitudes in the second sound compression wave produced by the same source, so that the ratio of intensities of the first and second sound waves emitted into He II by a variable temperature surface is much smaller than one for $T < T_\lambda$.[1,3,12] However, this disagrees with experiment[8,17] and in addition, the first sound is observed only when the power exceeds a critical value.

Figure 9 shows on top the oscilloscope traces of the arrival of the fundamental and reflected first sound pulses for $T = 2.12$ K, and on the bottom for first sound pulses at $T = 2.6$ K. The measurements were carried out in a cell of diameter 2 cm with a spacing $L = 0.3$ cm for $Q = 8$ W/cm^2 and $\tau = 1$ μs. It can be seen that in He II the amplitudes δT of the waves of first and second sound are close to each other in magnitude, but are of opposite sign, i.e., in the first sound wave $\delta T < 0$. The polarity change in transition from He II to He I corresponds to a sign change of β, and the ratio of the amplitudes of the pulses above and below T_λ is close to the ratio of the products of the quantities $\beta T/C_p$ for the same temperatures. The shapes of the first sound pulses is close to triangular, i.e., at distances smaller than 0.3 cm a first sound shock wave is formed in the liquid with a discontinuity on the wave front of the traveling plane pulse.

From this one can draw two conclusions: 1) Both in He I and in He II a compression wave propagates in the liquid.

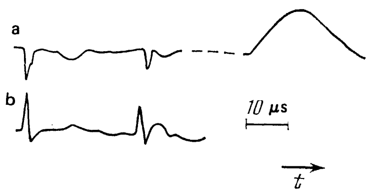

FIG. 9. a) The fundamental and reflected first sound pulses in He II at $T = 2.12$ K; b) first sound pulses in He I at $T = 2.6$ K (plane geometry, $L = 0.3$ cm, $Q = 8$ W/cm^2, $\tau = 1$ μs).

The excess pressure estimated according to the amplitude of the temperature oscillations in the wave is close to the saturated vapor pressure above the liquid. 2) The mechanism for the formation of compression waves in He II and He I is the same: a pulsed overheating of the interface layer of the liquid near T_λ and the formation of a gas film along the surface of the emitter. For the formation of a film it is necessary that the gas bubbles formed by the thermal fluctuations should succeed in growing and fusing into one during the lifetime of the pulse, i.e., the threshold power Q_c depends on the duration of the pulse. It follows from the relation (5) that for $\tau = 1$ μs and $T = 4.2$ K this requires a power of $Q_c \approx 200$ W/cm^2, but it is more likely that for $T < 4$ K the power Q_c decreases, so that as the temperature decreases the saturated vapor pressure decreases exponentially. In addition, one must take into account the possibility of an inhomogeneous superheating of parts of the heater on account of inhomogeneities of the film. (Reflection of a laser beam from the surface of a gas film formed at the locations of intensive recombination of electronic excitations on the surface of a semiconductor by laser pumping, and the propagation of first sound shock waves in He II, were observed in the experiments described in Ref. 18, 19. True, it is hard to estimate Q_c from the data of these experiments.)

It follows from Fig. 9 that the amplitude of the rarefaction wave is much smaller than the amplitude of compression wave, i.e., if a compression sound pulse is related to the formation and expansion of gas bubbles during the action of the pulse, then a film accumulates gradually and over a substantially longer time.

When one goes over to a pointlike emitter, in addition to the spherical waves of second sound we have observed spherical first sound shock waves. The dependence of the shape of the wave in He II and He I on the power level is shown in Figs. 10 a, b. Figure 10, c illustrates the change of shape of a pulse as the temperature of the bath changes. We attribute the decrease of the amplitude and the growth of noise to sound scattering by the gas bubbles. Since in He I it is important to minimize the scattering of sound waves on the bubbles formed in the volume of the freely boiling liquid, we have carried out these measurements at atmospheric pressure, which exceeds by several factors the saturated vapor pressure at $T < 3.5$ K.

In distinction from the second sound, where the shape of the pulses changes on passing through the temperature T_s (Fig. 6), in a divergent first sound wave only the polarity of the temperature oscillation is changed by transition through

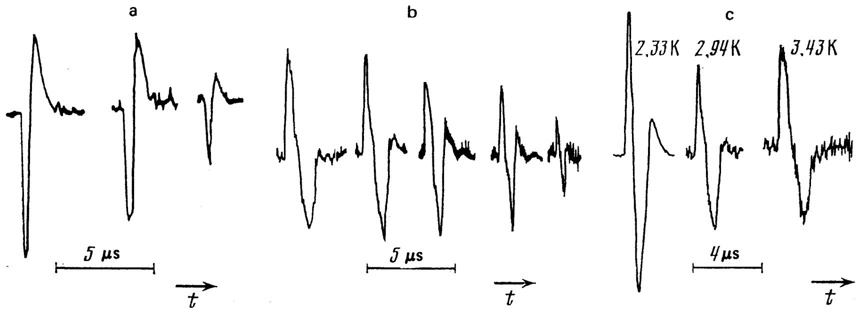

FIG. 10. The evolution of the shape of a spherical shock wave with the change in power of the exciting pulse of duration 0.1 μs (curves a, b) or of the temperature of the bath (curve c): a) He II, $T = 2.012$ K, $Q = 500, 400, 300$ 8 W/cm^2; b) He I, $T = 2.94$ K, $Q = 650, 500, 300, 240, 130$ 8 W/cm^2, the temperatures are indicated on the graphs.

T_λ, whereas the shape of the pulse, apart from sign, remains unchanged (Figs. 10, a, b).

The profile of the rarefaction waves in both second and first sounds differs in our experiments from the profile $v(r)$ shown in §95 of Ref. 1; according to Landau-Lifshitz the wave amplitude behind the shock front decreases slowly as $r \to 0$, and in Fig. 10 and in Figs. 5, and 6 the width of the rarefaction wave is close to that of the compression wave, and behind the rarefaction waves comes a small-amplitude compression wave if the damping in the volume is small. Of course, the radiation pattern of a source of finite size placed on a plane reflecting surface differs from that of a point source. However, Fig. 10 shows that the difference in shape of the front of the traveling wave from a sphere is not the most important feature. A decisive role is played by the properties of the medium and by phenomena occuring at the emitter-liquid interface at large power levels. Therefore additional theoretical investigations of the mechanisms of formation first-sound compression waves in liquid helium, and the formation of vortices in He II, when powerful short heat pulses are emitted seems to be of extreme interest. In the Introduction we have listed a number of other questions which arise in the study of the dynamics of motion of second sound shock waves in helium.

The authors are indebted to A. V. Lokhov for help with the measurements, to V. P. Mikheev and S. V. Iordanskiĭ for useful discussions, and to Yu. Z. Kovdre for useful remarks which led to an improvement of the text of the article.

[1]L. D. Landau and E. M. Lifshitz, Mekhanika sploshnykh sred (Mechanics of continuous media), Gostekhizdat, Moscow 1954; [Engl. Transl.: Fluid Mechanics, Pergamon Press, Oxford 1959].
[2]D. V. Osborne, Proc. Phys. Soc. (Lond.) **A64**, 114 (1951).
[3]I. M. Khalatnikov, Teoriya sverkhtekuchesti (Theory of superfluidity) Nauka, Moscow, 1971 [Engl. Transl. of older edition, Benjamin, NY 1965].
[4]A. J. Dessler and W. M. Fairbank, Phys. Rev. **104**, 6 (1956).
[5]J. C. Cummings, D. W. Schmidt, and W. Wagner, Phys. Fluids **21**, 713 (1978).
[6]M. O. Lutset, S. K. Nemirovskiĭ, and A. N. Tsoĭ, Zh. Eksp. Teor. Fiz. **81**, 249 (1981) [Sov. Phys. JETP **54**, 127 (1981)].
[7]A. I. Gulyaev, Zh. Eksp. Teor. Fiz. **57**, 59 (1969) [Sov. Phys. JETP **30**, 34 (1970)].
[8]A. Yu. Iznankin and L. P. Mezhov-Deglin, Pis'ma v ZhETF **29**, 755 (1979) [JETP Lett. **29**, 693 (1979)].
[9]L. P. Mezhov-Deglin, A. Yu. Iznankin, and V. P. Mineev, Pis'ma v ZhETF **32**, 217 (1980) [JETP Lett. **32**, 199 (1980)].
[10]A. Yu. Iznankin and L. P. Mezhov-Deglin, in Proceedings of the XXI All-Union low temperature physics conference, Khar'kov, 1980, vol. 4, p. 51.
[11]A. Yu. Iznankin and L. P. Mezhov-Deglin, in Proceedings of the XXII All-Union low temperature physics conference, Kishinev, 1982, vol. 4, p. 41.
[12]S. Putterman, Hydrodynamics of Superfluids, No. Holland, Amsterdam, 1974 [Russian Transl. Mir. Moscow, 1978].
[13]O. Tsukamoto and S. Kobayashi, Proc. Intl. Conf. LT-14, Amsterdam 1975, vol. 1. p. 305.
[14]W. F. Vinen, Proc. Phys. Soc. (Lond.) **A240**, 114 (1957).
[15]S. K. Nemirovskiĭ and A. N. Tsoi, Pis'ma v ZhETF **35**, 229 (1982) [JETP Lett. **35**, 286 (1982)].
[16]S. V. Iordanskiĭ, Zh. Eksp. Teor. Fiz. **48**, 708 (1965) [Sov. Phys. JETP **21**, 467 (1965)].
[17]M. Pomerantz, Phys. Rev. Lett. **26**, 362 (1971).
[18]I. V. Kavetskaya, M. N. Sibel'din, V. B. Stropatinskii, and V. A. Tsvetkov, Dokl. Akad. Nauk SSSR **224**, 559 (1979) [Sov. Phys. Doklady **24**, 37 (1979)].
[19]V. A. Tsvetkov, M. N. Sibel'din, V. B. Stropatinskii, and B. Etienne, Pis'ma v ZhETF **32**, 224 (1980) [JETP Lett. **32**, 206 (1980)].

Translated by M. E. Mayer